Perturbation of Retinoid Homeostasis Increases Malformation Risk in Embryos Exposed to Pregestational Diabetes

Short title: Retinoid homeostasis in diabetic embryopathy

Leo M.Y. Lee,[1,2,3] Maran B.W. Leung[1], Rachel C.Y. Kwok[1], Yun-Chung Leung[3], Chi-Chiu Wang[1,2], Peter J. McCaffery[4], Andrew J. Copp[5] and Alisa S.W. Shum[1]

[1]School of Biomedical Sciences, [2]Department of Obstetrics and Gynaecology, Faculty of Medicine, The Chinese University of Hong Kong, Hong Kong

[3]Department of Applied Biology and Chemical Technology, The Hong Kong Polytechnic University, Hong Kong

[4]Institute of Medical Sciences, University of Aberdeen, Aberdeen AB25 2ZD, United Kingdom

[5]Newlife Birth Defects Research Centre, Institute of Child Health, University College London, London WC1N 1EH, United Kingdom

Corresponding author:

Alisa S.W. Shum

School of Biomedical Sciences, The Chinese University of Hong Kong, Hong Kong

Tel: (852) 39436840   Fax: (852) 39420990   e-mail: alisa-shum@cuhk.edu.hk

(7 Figures, 1 Table, 7 Supplementary Figures, 3 Supplementary Tables)

1

ABSTRACT

Pregestational diabetes is highly associated with increased risk of birth defects. However, factors that can increase or reduce expressivity and penetrance of malformations in diabetic pregnancies remain poorly identified. All-*trans* retinoic acid (RA) plays crucial roles in embryogenesis. Here, we find that *Cyp26a1*, which encodes a key enzyme for catabolic inactivation of RA required for tight control of local RA concentrations, is significantly down-regulated in embryos of diabetic mice. Embryonic tissues expressing *Cyp26a1* show reduced efficiency of RA clearance. Diabetes-exposed embryos are thus sensitized to RA and more vulnerable to the deleterious effects of increased RA signalling. Susceptibility to RA teratogenesis is further potentiated in embryos with a pre-existing genetic defect of RA metabolism. Increasing RA clearance efficiency by a pre-conditioning approach can counteract the increased susceptibility to RA teratogenesis in embryos of diabetic mice. Our findings provide new insight into gene-environment interactions that influence individual risk in manifestation of diabetes-related birth defects, and shed light on the environmental risk factors and genetic variants for a stratified medicine approach to screen diabetic women of childbearing age and assess risk of birth defects during pregnancy.

Offspring of women with pregestational diabetes show markedly increased risk of birth defects (1). While the cause of diabetic embryopathy is known to be multifactorial, previous investigations mainly focussed on the effect of maternal diabetes alone on the embryo. Genetic and environmental factors that can influence expressivity and penetrance of congenital malformations in diabetic pregnancies remain far from clear (2,3). Interestingly, some malformations found in the offspring of diabetic mothers (4-6) are very similar to those anomalies in humans and animals arising from exposure to excess retinoids (vitamin A and its analogues) (7-9). For instance, a large-scale study of 18 population-based congenital anomaly registries shows that the odds ratio for caudal regression in diabetic versus non-diabetic pregnancy (odds ratio: 26.4; 95% confidence interval: 8.98-77.64) is well above other malformations (4), which strengthens the conclusion of previous studies that caudal regression is a characteristic anomaly associated with diabetic pregnancy (5,6). Caudal regression also commonly occurs with retinoid teratogenesis in animal studies (9-11).

Many of the functions of vitamin A in embryogenesis are mediated via its metabolite all-*trans* retinoic acid (RA), which is a key signalling molecule controlling the development of multiple organ systems. Different embryonic tissues/organs show variations in requirement for RA, thus tight regulation of local RA concentrations is critical to ensure precise levels of RA signalling required for normal embryo development. An important mechanism to control local RA concentrations is via catabolic inactivation by the CYP26 enzymes belonging to the cytochrome P450 family. Three *Cyp26* genes, namely *Cyp26a1*, *b1* and *c1*, are expressed in specific embryonic tissues and attenuate deleterious effects of excessive RA signalling. Among them, CYP26A1 is the key RA catabolizing enzyme in many tissues and the only subtype that

is expressed in the tailbud region of the embryo (12), where caudal regression arises (11). Homozygous deletion of *Cyp26a1* in mice results in lethality at mid-late gestation, with embryos exhibiting caudal truncation (13,14). Similarly, we and others have demonstrated that mouse embryos exposed to excess RA develop caudal truncation and various phenotypes, including specific renal, anorectal, caudal spinal cord and lower extremity malformations (10,11,15) commonly associated with caudal regression in humans (16,17). Moreover, we find that maternal diabetes potentiates the effect of RA to cause caudal regression in mice (18). This similarity in phenotypes resulting from genetic and environmental disturbances therefore led us to speculate that maternal diabetes may perturb embryonic CYP26A1 function in maintaining a tight regulation of local RA concentrations in specific tissues. We hypothesized that such tissues will be vulnerable to perturbation of RA levels and exhibit increased susceptibility to RA teratogenesis. Here, we provide evidence to support this hypothesis using a mouse model of pregestational diabetes. Notably, our findings show that interaction between a genetic predisposition and an environmental agent to disrupt RA homeostasis can potentiate maternal diabetes-induced deregulated RA catabolism in increasing malformation risk.

RESEARCH DESIGN AND METHODS

Animals

All animal experimentation was conducted following the guidelines set by The Chinese University of Hong Kong. Diabetes was induced in ICR female mice by streptozotocin injections according to our established protocols (18). Mice with blood glucose concentration ≥16.7 mmol/L were classified as manifestly diabetic (MD). Untreated, age-matched female ICR mice were employed as the non-diabetic (ND) control. Mice were kept in a 12:12 h light-dark cycle with the light cycle commenced at 11:00am. Pregnancies were obtained by timed mating for 2 h (9:00-11:00am) between MD/ND female ICR mice and male ICR mice, or male $Cyp26a1^{+/-}$ mice in 129/C57BL/6Cr/DBA mixed background (a gift from Prof. Hamada, 14). The time of finding a copulation plug at 11:00am was defined as embryonic day (E) 0. Mice were checked for blood glucose levels prior to embryo collection to confirm that MD mice remained diabetic during pregnancy (Supplementary Table 1).

Gene Expression

Whole embryos were subjected to *in situ* hybridization (ISH) for *Cyp26a1*, *Cyp26b1* or *Cyp26c1* with digoxygenin-labeled RNA probes (19). The mRNA expression levels of various genes were determined by real-time qRT-PCR. To minimize differences in expression levels due to variations in the developmental stage, only embryos within the same somite-range (9-10 somite-stage for E8 embryos; 19-21 somite-stage for E9 embryos) in each litter were collected. This criterion was adopted for embryo collection

in other experiments. For crossing between ICR male and ICR female mice, all embryos at appropriate somite-stage from the same litter were pooled as one sample. For crossing between $Cyp26a1^{+/-}$ male and ICR female mice, embryos were individually collected. After DNA genotyping of the yolk sac by PCR using primers as described (14), embryos of the same genotype ($Cyp26a1^{+/+}$ or $Cyp26a1^{+/-}$) from the same litter were pooled as one sample. Total RNA was extracted from the whole embryo or tailbud (defined as the caudal end of the embryo up to one somite-length posterior to the last somite) samples using the RNeasy Mini Kit (Favorgen). An equal amount of RNA (250 ng) was reverse-transcribed into first-strand cDNA using the High Capacity cDNA Reverse Transcription Kit (Applied Biosystems). The cDNA yielded from reverse transcription of 1.67 ng RNA was subjected to quantitative PCR using ABI 7900HT Fast Real-Time PCR system (Applied Biosystems), with SYBR Green PCR Master Mix (Applied Biosystems). *β-actin* was used as internal control for normalization. The PCR conditions and primer sequences were listed in Supplementary Table 2.

In Vitro RA Degrading Efficiency

Using an assay modified from Yamamoto (20), four tailbuds of E9 embryos from the same litter were pooled as one sample and lysed in 5 µl of DMEM by trituration with a pipette tip, followed by 5 cycles of freezing in liquid nitrogen and thawing in a water bath at $37^{o}C$ for 1 min. The whole lysate was added to 50 µl of a reaction mixture containing 50 nM all-*trans* RA (Sigma-Aldrich), with or without 1.6 mg/ml NADPH (cofactor of cytochrome P450 enzyme), 0.3 mg/ml DTT (reducing agent for optimal cytochrome P450 enzyme function) and CYP26 specific inhibitor R115866 (21) at a concentration of 1, 10 or 100 nM in a culture medium (DMEM supplemented with 10% fetal bovine

serum). The reaction mixture was then incubated in a 5% CO_2 incubator at 37^oC for 2 h, during which the exogenous RA in the medium was degraded by the RA catabolizing enzyme in the tailbud lysate. After incubation, the amount of RA remaining was determined by adding the reaction mixture, diluted 30-fold with the culture medium, in triplicate to a 96-well plate containing RA reporter cells, which are F9 cells transfected with a RA response element that drives β-galactosidase expression (22). Serially diluted RA standard solutions at concentrations from 10^{-6}M to 10^{-11}M were added in triplicate to the same 96-well plate. After culturing for 24 h, cells were stained with X-gal and the intensity of the blue product was measured using a microplate spectrophotometer. RA in the sample was quantified using a standard curve constructed with the serially diluted RA solutions (Supplementary Figure 1).

In Vivo Clearance of RA

To determine *in vivo* efficiency of RA clearance, at various time points post-injection of 50 mg/kg body weight of RA at E9, the tailbud was collected under dim yellow light. Tailbuds were individually placed in 300 μl of the culture medium added with 100 nM R115866 to inhibit endogenous CYP26 enzymes. After 24 h of incubation in 5% CO_2 at 37^oC, to allow maximum release of RA from the tailbud into the medium, RA in the medium was quantified using the RA reporter cell line. A preliminary study demonstrated that the culture conditions did not cause significant degradation of RA (Supplementary Figure 2). To validate that RA measured using the RA reporter cell line measures RA released from tissues that can modulate RA levels, the tailbud of E9 embryos was collected 3 h post-injection of RA. The midbrain, which does not express any *Cyp26*

genes in untreated or RA-treated conditions, was also collected from these embryos as a control. Tissues from the same litter were pooled as one sample. RA in the sample was quantified using HPLC (23).

Detection of Bioactive RA in Tailbud

The caudal-most portion of the tailbud of E9 embryo of MD and ND mice was excised under dim yellow light and individually placed on top of RA reporter cells grown on a 96-well plate in the culture medium added with 100 nM R115866 to inhibit endogenous CYP26 enzymes. After 24 h of culture, cells were stained with X-gal. The number of positively stained cells around the tailbud explant was counted under a stereomicroscope.

Susceptibility to RA Teratogenesis

The teratogenic effect of RA is dose- and stage-dependent (9). To determine the susceptibility to RA teratogenesis, MD or ND mice at E8 or E9 received an intraperitoneal injection of 25 mg/kg RA or equivalent volume of suspension vehicle (peanut oil) as a control, and their embryos were examined at E13. Embryos treated with RA at E9 were examined for the extent of caudal truncation, which was expressed as the ratio of tail length to crown-rump length as used in our previous studies (18). Embryos treated with RA at E8 were examined for exencephaly and spina bifida. Near-term E18 fetuses maternally treated with 40 mg/kg RA at E9 were examined for various types of renal malformations as described in our previous studies (24). Maternal pre-conditioning with low dose RA (0.625 or 1.25 mg/kg) or suspension vehicle (peanut oil) as a control was achieved by oral gavage 2 h before receiving intraperitoneal injection of teratogenic

dose of RA.

Statistics

Statistical differences between two groups were analyzed by unpaired Student's *t* test. Differences between multiple groups of data were analysed by one-way ANOVA, followed by Bonferroni post-hoc test, or by using Contrast test for assessing extent of differences. Dose response was analyzed by linear regression. The best-fit curves were compared by nonlinear regression. Data were presented as mean ± SEM, with $P < 0.05$ considered as statistically significant. All statistical analyses were conducted using the *SPSS* software (SPSS Inc.), except nonlinear regression analysis, which was conducted using the *Prism* software (GraphPad Software).

RESULTS

Cyp26a1 Expression Levels and RA Degrading Efficiency are Reduced in Embryos of Diabetic Mice

During early mouse post-implantation development, *Cyp26a1* is initially expressed in the headfold mesenchyme (Fig. 1*A*), and then extends to the caudal neural plate and primitive streak (Fig. 1*B*). As development proceeds, *Cyp26a1* expression persists at the caudal end (Fig. 1*C* and *D*), now called the tailbud, which contains progenitor cells for forming various posterior structures. Rostrally, it is expressed in the craniofacial, cervical and branchial arch mesenchyme (Fig. 1*C*). Embryos of manifestly diabetic (MD) mice exhibit a significant decrease in *Cyp26a1* mRNA transcripts in all of these regions compared with embryos of non-diabetic (ND) mice (Fig. 1*A-E*). In contrast, *Cyp26b1* and *Cyp26c1* are expressed predominantly in the cranial region but not in the tailbud (Fig. 1*F* and *H*), and show no significant difference in expression levels between embryos of MD and ND mice (Fig. 1*G* and *I*).

To determine whether a decrease in *Cyp26a1* expression results in reduced efficiency of RA catabolism, we employed an *in vitro* assay to compare the RA degrading efficiency of the tailbud, which exclusively expresses *Cyp26a1*, but not *Cyp26b1* and *Cyp26c1*, from E9 embryos of MD and ND mice. Results showed that only a low level of RA degrading activity was detected when tailbud lysate alone was applied (Fig. 2*A*). However, in the presence of NADPH and DTT for optimal activity of CYP26 enzymes, 66% of added RA was degraded within 2 h. In contrast, co-treatment with 1-100 nM of R115866, a potent CYP26-specific inhibitor (21), resulted in a

significant dose-dependent inhibition of RA degradation. Notably, while there was no significant difference in the protein content of the excised tailbuds from embryos of MD and ND mice (Supplementary Figure 3), tailbud lysate of the MD group exhibited only 45% of activity of the ND group.

To further compare the efficiency of *in vivo* clearance of RA, MD and ND mice were injected with an exogenous dose of 50 mg/kg RA at E9, followed by measurement of RA in individual tailbuds at hourly intervals using the RA reporter cell line (Fig. 2*B*), which showed results comparable with quantification of RA using HPLC (Supplementary Table 3). Despite a similar response time-course in MD and ND groups, the amount of RA in tailbuds of the MD group was significantly higher than the ND group at all time-points studied (Fig. 2*B*). Moreover, by determining the area under the concentration-time curve (AUC), which is considered as the most appropriate pharmacokinetic correlate of embryotoxicity of RA (25), there was a two-fold difference between MD (AUC_{0-8h}: 25.59 nM x h, calculated by the *Prism 5* software, GraphPad Software) and ND (AUC_{0-8h}: 12.70 nM x h) groups, implying that the efficiency of *in vivo* RA clearance in tailbuds of diabetes-exposed embryos was reduced by 50%. In contrast, the E9 midbrain, which does not express any of the three *Cyp26* genes in both untreated and RA-treated conditions (Supplementary Figure 4*A*), exhibited no differences in RA levels between embryos of MD and ND mice at 3 h post-injection of RA (Supplementary Figure 4*B*).

RA Levels are Increased in Tailbuds of Embryos of Diabetic Mice

To determine whether reduction in RA degrading efficiency would lead to a rise in

endogenous RA levels, we excised the caudal-most part of the tailbud (Fig. 3*A*) furthest away from the RA source in adjacent trunk tissues, and put it directly on the RA reporter cells to detect bioactive RA release (22). Reporter cells exposed to RA expressed β-galactosidase and turned blue with X-gal staining. There were hardly any positively stained cells around tailbuds from embryos of ND mice (Fig. 3*B* and *C*), which agrees with previous findings that the tailbud is normally devoid of RA (26). However, stained cells were observed around more than half the tailbuds from embryos of MD mice. The number of stained cells varied from under 10 to over 40, implying a varying magnitude of elevation of RA level in tailbuds of diabetes-exposed embryos.

Several genes including *Fgf8*, *Wnt3a* and *Cdx2* are indispensable key players in caudal development (27). Excessive RA has been demonstrated to down-regulate these genes and cause axial truncation (11,26,28). However, of these genes, only *Fgf8* was significantly down-regulated in the tailbud of embryos of MD mice (Fig. 4*A*). It is possible that the magnitude of increase in RA levels may not have reached the threshold for causing detectable alteration in the expression of some of these genes. We therefore challenged embryos with 50 mg/kg of RA to test whether deregulated catabolism of RA would sensitize embryos of MD mice to RA. At 4 h post-injection of RA, there was a dramatic increase in mRNA levels of *Cyp26a1* in the tailbud (Fig. 4*B*), showing that *Cyp26a1* is highly inducible by RA. However, the magnitude of up-regulation of *Cyp26a1* in tailbuds of the MD group was significantly less than the ND group ($P < 0.05$, Contrast test), which further exacerbated the difference between these two groups. Concomitantly, there was a marked down-regulation of *Fgf8*, with expression levels in tailbuds of the RA-treated MD group reduced to less than one-third of the ND group without RA treatment (Fig. 4*C*). Consistent with our previous findings (18), though there

was no difference in *Wnt3a* expression levels between tailbuds of MD and ND groups at steady-state (Fig. 4*A*), upon RA challenge, *Wnt3a* was down-regulated to a significantly greater extent in tailbuds of the MD group than the ND group (Fig. 4*C*). Similarly, the MD group showed increased propensity to RA-induced down-regulation of *Cdx2*.

RA action is mediated via transactivation by retinoic acid receptors (Rar) that heterodimerize with retinoid X receptors (Rxr). In the mouse embryo, Rarγ and Rxrα mediate the teratogenic effect of RA in inducing caudal truncation (29,30). However, there were no differences in expression levels of *Rarγ* and *Rxrα* between tailbuds of embryos of ND and MD mice at steady-state (Fig. 4*A*) or 4 h post-injection of RA (Fig. 4*C*). Together, these findings support the idea that enhanced down-regulation of caudal regulatory genes in tailbuds of embryos of MD mice is due to increased RA levels resulting from reduced efficiency of RA degradation, rather than secondary to differences in efficiency of transactivation via the RA receptors.

Genetic Reduction of *Cyp26a1* Exacerbates Susceptibility of Embryos of Diabetic Mice to RA Teratogenesis

We asked whether a decrease in *Cyp26a1* expression leads directly to reduced efficiency of RA clearance, and whether functional loss of *Cyp26a1* could interact with the maternal diabetic environment to influence RA degrading efficiency and susceptibility to RA teratogenesis. To investigate these questions, we crossed $Cyp26a1^{+/-}$ male mice with MD or ND female mice. We hypothesized that $Cyp26a1^{+/-}$ mutant embryos would exhibit a lower RA degrading efficiency than their $Cyp26a1^{+/+}$ wild-type littermates and that exposure to maternal diabetes would exacerbate these genetic differences.

Indeed, E9 embryos from different genotype-maternal environment combinations

showed prominent differences in *Cyp26a1* levels (Fig. 5*A*). The *Cyp26a1* mRNA levels

in tailbuds of *Cyp26a1*$^{+/-}$ embryos of MD mice were reduced to half of the level in

Cyp26a1$^{+/+}$ embryos of ND mice (Fig. 5*B*), with a corresponding decrease in

CYP26-mediated RA degrading efficiency (Fig. 5*C*). When RA levels were raised, via

maternal challenge with 25 mg/kg of RA, a 50% reduction in *Cyp26a1* expression levels

and RA degrading efficiency in tailbuds of *Cyp26a1*$^{+/-}$ embryos of MD mice resulted in

exposure to an eight-fold higher effective concentration of RA in comparison to tailbuds

of *Cyp26a1*$^{+/+}$ embryos of ND mice (Fig. 5*D*). This effect was noted 3 h after RA

injection, when accumulation of RA had reached peak level (Fig. 2*B*). In agreement with

these findings, *Cyp26a1*$^{+/-}$ embryos of MD mice were most sensitized to RA-induced

caudal truncation (Supplementary Figure 5), as indicated by the smallest ratio of tail

length (TL) to crown-rump length (CRL) (Fig. 5*E*). TL/CRL ratio was used as a

'surrogate' both for regression of multiple caudal structures in mice and for the analogous

'caudal regression' process that affects species without tails, such as humans. In addition

to caudal truncation, renal malformations are commonly associated with caudal regression

(15,16). Indeed, we also found a twelve-fold increase in incidence (Fig. 5*F*) and severity

(Table 1) of renal malformations in near-term *Cyp26a1*$^{+/-}$ fetuses exposed to maternal

diabetes compared with wild-type fetuses in non-diabetic pregnancy when being

challenged with a teratogenic dose of RA.

Enhancing RA Degrading Efficiency Counteracts Increased Susceptibility to RA

Teratogenesis Induced by Maternal Diabetes

Cyp26a1 is highly RA-inducible, as it contains multiple RA response elements (31). Thus,

as a proof-of-principle, we attempted to 'pre-condition' embryos of MD mice by using an

exogenous sub-teratogenic RA dose to up-regulate *Cyp26a1* expression, in order to determine whether pre-conditioning could lead to a protective effect against RA teratogenesis. Previous findings showed that maternal oral administration of 2.5 mg/kg RA is sufficient to achieve near full rescue of mid-gestation mouse embryos lacking Raldh2, the principal RA synthetic enzyme (32). Therefore, we pre-conditioned pregnant mice with 0.625 or 1.25 mg/kg RA via oral feeding. These dosages are far below the teratogenic concentration range, but yielded a dose-dependent increase in *Cyp26a1* mRNA levels in tailbuds of embryos by 2 h after administration (Fig. 6*A*). Notably, supplementation with 0.625 mg/kg RA did not induce changes in *Fgf8*, *Wnt3a* and *Cdx2* expression (Supplementary Figure 6), but up-regulated the expression of *Cyp26a1* in tailbuds of the MD group to a level similar to that of the ND group fed with vehicle (Fig. 6*A*), with a concomitant normalization of RA degrading efficiency (Fig. 6*B*). Then, when maternally challenged with an intraperitoneal injection of a teratogenic dose of 25 mg/kg RA, we found the severity of caudal truncation to be significantly reduced, as shown by the significantly higher TL/CRL ratio in embryos of RA-pre-conditioned mice than in embryos from vehicle-fed mice in both MD and ND conditions (Fig. 6*C*). Even the higher (1.25 mg/kg) pre-conditioning dose of RA was non-teratogenic and by itself did not affect the TL/CRL ratio of the embryo. While it could have had other effects on the embryo, in addition to up-regulating *Cyp26a1*, the highly comparable pattern of dose-dependent up-regulation of *Cyp26a1* and dose-dependent increase in the TL/CRL ratio, in the absence of changes in the key caudal regulatory genes, suggests a specific effect of pre-conditioning. These findings support the idea that pre-conditioning the embryo via enhancing RA degrading efficiency can offer a protective effect against RA teratogenesis and abolish the increased propensity of embryos from diabetic pregnancy to

RA-induced caudal truncation.

Amongst the most frequent congenital anomalies associated with maternal diabetes are neural tube defects (NTDs) (4). Expression levels of *Cyp26a1* in the cranial mesenchyme and the caudal neural plate are prominently reduced in E8 embryos of MD mice (Fig. 1*B*). Moreover, *Cyp26a1*$^{-/-}$ embryos exhibit exencephaly and spina bifida (13,14), suggesting the importance of CYP26A1 enzyme in protecting these tissues from the deleterious effects of ectopic RA signalling. We found that injection of 25 mg/kg of RA at E8 induced around 6.7% exencephaly (Fig. 7*A*) and 4.4% spina bifida (Fig. 7*B*) in *Cyp26a1*$^{+/+}$ embryos of ND mice. However, the incidence of RA-induced exencephaly and spina bifida was markedly increased by six- and seven-fold respectively in *Cyp26a1*$^{+/+}$ embryos exposed to diabetes. Similar trend was found in embryos of ICR x ICR background (Supplementary Figure 7). The penetrance of NTDs was further exacerbated to 75.0% exencephaly and 71.3% spina bifida in *Cyp26a1*$^{+/-}$ embryos of MD mice with a pre-existing genetic defect of RA catabolism. Similar to caudal truncation, the increase in susceptibility to RA-induced exencephaly and spina bifida caused by maternal diabetes was significantly reduced when embryos were pre-conditioned by maternal feeding of low dose RA. Together, these findings support the idea that deregulated RA catabolism resulting from reduced levels of *Cyp26a1* expression acts to sensitize embryos of diabetic pregnancy to fluctuations in RA levels.

DISCUSSION

In the present study, we found that the embryonic expression of the key RA catabolizing enzyme *Cyp26a1* is significantly down-regulated under maternal diabetes. This leads to a decrease in RA inactivation efficiency and enhances the deleterious effect of excessive RA signalling on key caudal regulatory genes, such as *Fgf8*, *Wnt3a* and *Cdx2*, which are required for continued axial elongation (27). We previously demonstrated that enhanced RA-induced down-regulation of *Wnt3a* exacerbated apoptosis in the tailbud of mouse embryos exposed to a diabetic or hyperglycemic condition, leading to premature termination of caudal development (18,33). This resulted in absence of lower vertebrae, imperforate anus, clubfeet, renal and caudal spinal cord malformations, all of which are commonly associated with caudal regression (10,11,15-17).

The most frequent anomalies in pregnancies complicated by pregestational diabetes are NTDs and congenital heart defects (CHDs) (4,5). Results of this study support the idea that a decrease in *Cyp26a1* expression also significantly increases the propensity of embryos from diabetic pregnancy to exencephaly and spina bifida when RA homeostasis is perturbed. Although we have not examined heart development, *Cyp26a1* is expressed in the cardiac neural crest cells, primitive heart tube and outflow tract, and *Cyp26a1*^{-/-} embryos exhibit CHDs (13,14). Specific subgroups of CHD associated with improper RA signalling (8,9) are highly similar to those showing increased frequencies in the offspring of mothers with pregestational diabetes (4,34). As tight regulation of RA signalling is critical for many developmental processes, deregulated RA catabolism in early embryonic life can perturb the development of multiple organ systems, which is in line with the finding that specific multiple congenital anomalies are common in affected

offspring of mothers with pregestational diabetes (4,5).

In our diabetic mouse colony, around 5% of embryos developed NTDs. However, there are large variations in congenital malformation frequencies between different laboratories, with the frequency of NTDs reaching over 50% in some reports (35). While genetic background affects the susceptibility to diabetic embryopathy (2,36), recent studies demonstrate that different types of rodent chow could significantly alter the frequency of NTDs in embryos of diabetic mice, which supports the idea that maternal diet is an important modifier of penetrance of malformation (3). Individual malformation risk will therefore depend on the interaction between genetic and environmental influences, which affects the developmental threshold of gene expression for normal development.

Many genetic and environmental factors can affect embryonic RA homeostasis and signalling pathways to potentiate the effect of maternal diabetes in increasing malformation risk in the offspring. In humans, genetic polymorphisms of *CYP26A1* that exhibit significantly lower degrading efficiency of RA have been identified (37,38). Duplication and polymorphisms of human *ALDH1A2* gene (encoding the principal RA synthetic enzyme during embryogenesis) are associated with increase in serum RA levels (39) and various types of congenital anomalies including CHDs and NTDs (40). Thus, common genetic variants involved in RA metabolism and signalling pathways could potentially be used as markers to identify diabetic pregnancies with increased malformation risk.

Retinoids are recognized human teratogens (41). Various forms of retinoids are in clinical use or under study for treatment of a variety of diseases, including skin disorders, obesity, diabetes and related complications (42). A well-known example is isotretinoin

(13-*cis* RA) prescribed for treatment of severe acne. It has been shown that the teratogenic threshold for isotretinoin is much lower in humans (0.5 mg/kg) (43) than in mice (100 mg/kg) (44). Human embryos are highly sensitive to isotretinoin, with a pattern of malformations (8) similar to that seen in animals exposed to all-*trans* RA teratogenesis (9). In fact, the teratogenic effect of 13-*cis* RA has been demonstrated in animals and suggested for humans to be mediated via its conversion to all-*trans* RA, which then binds to the nuclear RA receptors to regulate gene expression (45). Moreover, our previous (18) and present studies show that maternal diabetes can enhance RA teratogenicity. Thus the teratogenic threshold for isotretinoin in embryos of women with pregestational diabetes may be even lower than the 0.5 mg/kg figure previously quoted (43).

Other than direct exposure to retinoids, medications, such as the anti-convulsant valproic acid, and fluconazole for treating fungal and yeast infections, have been shown to increase embryonic RA levels and induce malformations (46,47). Maternal smoking may also impose increased risk since recent studies suggest that the teratogenic effect of nicotine on embryonic development is highly associated with suppression of *Cyp26a1* and perturbation of RA signalling (48). In fact, many chemicals can modulate RA homeostasis. As such, neural tube and axial defects mediated by modulation of RA homeostasis is proposed to be adopted as an Adverse Outcome Pathway (AOP) framework for assessing developmental toxicity of chemicals (49).

There is a global trend that type 2 diabetes increasingly affects children and adolescents (50). As the prevalence of diabetes in women of childbearing age continues to rise, the number of pregnancies complicated by pregestational diabetes is likely to increase exponentially. The partial penetrance and variable expressivity of diabetic

embryopathy underscore its multifactorial nature, implicating interactions between genetic make-up of the embryo, maternal factors and environmental influence. It is therefore of utmost importance to identify risk factors so as to reduce malformations in diabetic pregnancy. The present study is the first to show that RA catabolism is deregulated in embryos exposed to diabetes and suggests that pregnancies of diabetic women may be more vulnerable to perturbation in RA homeostasis and signalling. This may highlight the need to be cautious in assessing the upper safe levels of drugs, supplements and potential teratogens for women with pregestational diabetes, particularly those that have effects on RA homeostasis and signalling. Association studies should be conducted to determine whether specific genetic variants or peri-conceptional exposure to environmental agents that perturb RA homeostasis and signalling could be potentiation factors that increase individual malformation risk in the offspring of diabetic mothers. Identifying these targets could contribute to genetic screening and preventive healthcare for diabetic women with childbearing potential. Furthermore, as a proof-of-principle, we have demonstrated the protective effect of correcting RA catabolism in embryos of diabetic mice. This finding may form the basis for developing stratified medicine to reduce the risk of congenital anomalies in pregnancies complicated by pregestational diabetes.

Duality of Interest. No potential conflicts of interest relevant to this article were reported.

Author Contributions. L.M.Y.L. researched data and wrote the manuscript. M.B.W.L. and R.C.Y.K. researched data. Y.C.L. provided technical advice and contributed research materials. C.C.W contributed to discussion. P.J.M. provided technical advice, contributed research materials and edited the manuscript. A.J.C. contributed to discussion and edited the manuscript. A.S.W.S. designed the study and wrote the manuscript. A.S.W.S. is the guarantor of this work, and as such, had full access to all the data in this study and takes responsibility for the integrity of the data and the accuracy of the data analysis.

References

1. Correa A, Gilboa SM, Besser LM, et al. Diabetes mellitus and birth defects. Am J Obstet Gynecol 2008;199:237.e1-9
2. Pani L, Horal M, Loeken MR. Polymorphic susceptibility to the molecular causes of neural tube defects during diabetic embryopathy. Diabetes 2002;51:2871-2874
3. Kappen C, Kruger C, MacGowab J, Salbaum JM. Maternal diet modulates the risk for neural tube defects in a mouse model of diabetic pregnancy. Reprod Toxicol 2011;31:41-49
4. Garne E, Loane M, Dolk H, et al. Spectrum of congenital anomalies in pregnancies with pregestational diabetes. Birth Defects Res A Clin Mol Teratol 2012;94:134-140
5. Martinez-Frias ML. Epidemiological analysis of outcomes of pregnancy in diabetic mothers: identification of the most characteristic and most frequent congenital anomalies. Am J Med Genet 1994;51:108-113
6. Kucera J. Rate and type of congenital anomalies among offspring of diabeticwomen. J Reprod Med 1971;7:73-82
7. Rothman KJ, Moore LL, Singer MR, Nguyen US, Mannino S, Milunsky A. Teratogenicity of high vitamin A intake. N Engl J Med 1995;333:1369-1373
8. Lammer EJ, Chen DT, Hoar RM, et al. Retinoic acid embryopathy. N Engl J Med 1985;313:837-841
9. Shenefelt RE. Morphogenesis of malformations in hamsters caused by retinoic acid: relation to dose and stage at treatment. Teratology 1972;5:103-118
10. Padmanabhan R. Retinoic acid-induced caudal regression syndrome in the mouse fetus. Reprod Toxicol 1998;12:139-151
11. Shum AS, Poon LL, Tang WW, et al. Retinoic acid induces down-regulation of Wnt-3a, apoptosis and diversion of tailbud cells to a neural fate in the mouse embryo. Mech Dev 1999;84:17-30
12. Fujii H, Sato T, Kaneko S, et al. Metabolic inactivation of retinoic acid by a novel P450 differentially expressed in developing mouse embryos. EMBO J 1997;16:4163-4173
13. Abu-Abed S, Dollé P, Metzger D, Beckett B, Chambon P, Petkovich M. The retinoic acid-metabolizing enzyme, CYP26A1, is essential for normal hindbrain patterning, vertebral identity, and development of posterior structures. Genes Dev 2001;15:226-240
14. Sakai Y, Meno C, Fujii H, et al. The retinoic acid-inactivating enzyme CYP26 is essential for establishing an uneven distribution of retinoic acid along the anterio-posterior axis within the mouse embryo. Genes Dev 2001;15:213-225
15. Tse HK, Leung MB, Woolf AS, et al. Implication of Wt1 in the pathogenesis of nephrogenic failure in a mouse model of retinoic acid-induced caudal regression syndrome. Am J Pathol 2005;166:1295-1307
16. Duhamel B. From the mermaid to anal imperforation: the syndrome of caudal regression. Arch Dis Child 1961;36:152-155
17. Pang D. Sacral agenesis and caudal spinal cord malformations. Neurosurgery 1993;32:755-778
18. Chan BW, Chan KS, Koide T, et al. Maternal diabetes increases the risk of caudal regression caused by retinoic acid. Diabetes 2002;51:2811-2816

19. Wilkinson DG. Whole mount in situ hybridization of vertebrate embryos. In situ hybridization: A Practical Approach, IRL Press, Oxford. 1992;75-83

20. Yamamoto M, Dräger UC, McCaffery P. A novel assay for retinoic acid catabolic enzymes shows high expression in the developing hindbrain. Brain Res Dev Brain Res 1998;107:103-111

21. Stoppie P. R115866 inhibits all-trans-retinoic acid metabolism and exerts retinoidal effects in rodents. J Pharmacol Exp Ther 2000;293:304-312

22. Wagner M, Han B, Jessell TM. Regional differences in retinoid release from embryonic neural tissue detected by an in vitro reporter assay. Development 1992;116:55-66

23. Schmidt CK, Brouwer A, Nau H. Chromatographic analysis of endogenous retinoids in tissues and serum. Anal Biochem 2003;315:36-48

24. Lee LM, Leung CY, Tang WW, et al. A paradoxical teratogenic mechanism for retinoic acid. Proc Natl Acad Sci U S A 2012;109:13668-13673

25. Tzimas G, Thiel R, Chahoud I, Nau H. The area under the concentration-time curve of all-trans-retinoic acid is the most suitable pharmacokinetic correlate to the embryotoxicity of this retinoid in the rat. Toxicol Appl Pharmacol 1997;143:436-444

26. Iulianella A, Beckett B, Petkovich M, Lohnes D. A molecular basis for retinoic acid-induced axial truncation. Dev Biol 1999;205:33-48

27. Neijts R, Simmini S, Giuliani F, van Rooijen C, Deschamps J. Region-specific regulation of posterior axial elongation during vertebrate embryogenesis. Dev Dyn 2014;243:88-98

28. Kumar S, Duester G. Retinoic acid controls body axis extension by directly repressing Fgf8 transcription. Development 2014;141:2972-2977

29. Lohnes D, Kastner P, Dierich A, Mark M, LeMeur M, Chambon P. Function of retinoic acid receptor gamma in the mouse. Cell 1993;73:643-658

30. Kastner P, Mark M, Ghyselinck N, et al. Genetic evidence that the retinoid signal is transduced by heterodimeric RXR/RAR functional units during mouse development. Development 1997;124:313-326

31. Zhang Y, Zolfaghari R, Ross AC. Multiple retinoic acid response elements cooperate to enhance the inducibility of CYP26A1 gene expression in liver. Gene 2010;464:32-43

32. Niederreither K, Subbarayan V, Dollé P, Chambon P. Embryonic retinoic acid synthesis is essential for early mouse post-implantation development. Nat Genet 1999;21:444-448

33. Leung MB, Choy KW, Copp AJ, Pang CP, Shum AS. Hyperglycaemia potentiates the teratogenicity of retinoic acid in diabetic pregnancy in mice. Diabetologia 2004;47:515-522

34. Lisowski LA, Verheijen PM, Copel JA, et al. Congenital heart disease in pregnancies complicated by maternal diabetes mellitus. An international clinical collaboration, literature review, and meta-analysis. Herz 2010;35:19-26

35. Fine EL, Horal M, Chang T, Fortin G, Loeken MR. Evidence that elevated glucose causes altered gene expression, apoptosis, and neural tube defects in a mouse model of diabetic pregnancy. Diabetes 1999;48:2454-2562

36. Ejdesjö A, Wentzel P, Eriksson UJ. Genetic and environmental influence on diabetic rat embryopathy. Am J Physiol Endocrinol Metab 2011;300:E454-467

37. Lee SJ, Perera L, Coulter SJ, Mohrenweiser HW, Jetten A, Goldstein JA. The discovery of new coding alleles of human CYP26A1 that are potentially defective in the metabolism of all-trans retinoic acid and their assessment in a recombinant cDNA expression system. Pharmacogenet Genomics 2007; 17:169-180

38. Rat E, Billaut-Laden I, Allorge D, et al. Evidence for a functional genetic polymorphism of the human retinoic acid-metabolizing enzyme CYP26A1, an enzyme that may be involved in spina bifida. Birth Defects Res A Clin Mol Teratol 2006;76:491-498

39. El Kares R, Manolescu DC, Lakhal-Chaieb L, et al. A human ALDH1A2 gene variant is associated with increased newborn kidney size and serum retinoic acid. Kidney Int 2010;78:96-102

40. Deak KL, Dickerson ME, Linney E, et al. Analysis of ALDH1A2, CYP26A1, CYP26B1, CRABP1, and CRABP2 in human neural tube defects suggests a possible association with alleles in ALDH1A2. Birth Defects Res A Clin Mol Teratol 2005;73:868-875

41. Soprano DR, Soprano KJ. Retinoids as teratogens. Annu Rev Nutr 1995;15:111-132

42. Villarroya F, Iglesias R, Giralt M. Retinoids and retinoid receptors in the control of energy balance: novel pharmacological strategies in obesity and diabetes. Curr Med Chem 2004;11:795-805

43. Rosa FW, Wilk AL, Kelsey FO. Teratogen update: vitamin A congeners. Teratology 1986;33:355-364

44. Kraft JC, Kochhar DM, Scott WJ, Nau H. Low teratogenicity of 13-cis-retinoic acid (isotretinoin) in the mouse corresponds to low embryo concentrations during organogenesis: comparison to the all-trans isomer. Toxicol Appl Pharmacol 1987;87:474-482

45. Nau H. Teratogenicity of isotretinoin revisited: species variation and the role of all-trans-retinoic acid. J Am Acad Dermatol 2001;45:S183-187

46. Chuang CM, Chang CH, Wang HE, et al. Valproic acid downregulates RBP4 and elicits hypervitaminosis A-teratogenesis - a kinetic analysis on retinol/retinoic acid homeostatic system. PLoS One 2012;7:e43692

47. Di Renzo F, Broccia ML, Giavini E, Menegola E. Citral, an inhibitor of retinoic acid synthesis, attenuates the frequency and severity of branchial arch abnormalities induced by triazole-derivative fluconazole in rat embryos cultured in vitro. Reprod Toxicol 2007;24:326-332

48. Feltes BC, de Faria Poloni J, Notari DL, Bonatto D. Toxicological effects of the different substances in tobacco smoke on human embryonic development by a systems chemo-biology approach. PLoS One 2013;8:e61743

49. Tonk EC, Pennings JL, Piersma AH. An adverse outcome pathway framework for neural tube and axial defects mediated by modulation of retinoic acid homeostasis. Reprod Toxicol 2015;55:104-113

50. Reinehr T. Type 2 diabetes mellitus in children and adolescents. World J Diabetes 2013;4:270-281

Table 1. Frequency of various phenotypes (categorized according to the severity of malformations) in E18 *Cyp26a1* heterozygous null (+/-) and wild-type (+/+) fetuses from non-diabetic (ND) and manifestly diabetic (MD) mice induced by *in vivo* challenge with 40 mg/kg RA at E9

Maternal state	ND		MD	
Genotype of fetuses	+/+	+/-	+/+	+/-
No. of litters	11		11	
No. of live fetuses	68	61	48	49
Two normal kidneys	91.2%	80.3%	62.5%	36.7%
Unilateral non-agenesis renal malformations (*contralateral kidney being normal)*	2.9%	9.8%	16.7%	26.5%
Bilateral non-agenesis renal malformations	2.9%	8.2%	12.5%	10.2%
Unilateral renal agenesis (*solitary kidney being normal*)	1.5%	1.6%	0	8.2%
Unilateral renal agenesis (*solitary kidney with non-agenesis malformations*	1.5%	0	4.2%	6.1%
Bilateral renal agenesis	0	0	4.2%	12.2%

FIGURE LEGENDS

Figure 1 - Embryos of diabetic mice exhibit specific down-regulation of *Cyp26a1*. *A-D,F* and *H*: Whole-mount ISH patterns of *Cyp26* genes in embryos of manifestly diabetic (MD) mice compared with those of non-diabetic (ND) mice. *Cyp26a1* mRNA transcripts are seen in extraembryonic endoderm (red arrowhead) and headfold mesenchyme (yellow arrowhead) of E7 conceptuses (*A*), cranial mesenchyme (green arrowhead) and caudal neural plate (orange arrowhead) of E8 embryos (*B*), craniofacial, cervical and branchial arch mesenchyme (circled) (*C*), and tailbud (blue arrowhead) of E9 embryos (*D*). *Cyp26b1* (*F*) and *Cyp26c1* (*H*) are expressed in the cranial but not in the tailbud region of E9 embryos. At least 20 embryos from 5-6 litters were examined for each group. Scale bar = 0.05 mm (*A*), 0.1 mm (*B*), 0.7 mm (*C*), 0.2 mm (*D*), 0.7 mm for whole embryo and 0.35 mm for caudal region (*F* and *H*). *E,G,I*: Quantification of mRNA levels of *Cyp26a1* (*E*), *Cyp26b1* (*G*) and *Cyp26c1* (*I*), normalized to *β-actin*, and expressed relative to ND, which was set as 1 (*n* = 5 from 5 litters). *$P < 0.05$, Student's *t* test. Error bars represent mean ± SEM.

Figure 2 - Embryos of diabetic mice show reduced efficiency of RA catabolism. *A*: *In vitro* RA degrading efficiency, presented as % of RA in the medium being degraded by the tailbud lysate, in the presence or absence of cofactor (NADPH) and reducing agent (DTT) for optimal activity of CYP26 enzymes, and varying concentrations of R115866 (CYP26 inhibitor) (*n* = 18 in ND and MD groups with NADPH-DTT, and *n* = 3-9 in other groups, from 20 ND and 18 MD litters). *$P < 0.001$, Student's *t* test; [†]$R^2 = 0.742$

and $P = 0.001$, linear regression. *B*: *In vivo* RA clearance measured as the amount of RA released from individual tailbuds, using a RA reporter cell line, at hourly intervals after injection of 50 mg/kg RA at E9 ($n = 16\text{-}42$ from 3-8 litters). *$P < 0.001$ vs ND; Student's *t* test and nonlinear regression. Error bars represent mean ± SEM.

Figure 3 - Tailbuds of E9 embryos of diabetic mice have increased levels of endogenous RA detected using a RA reporter cell line. *A*: Figure to illustrate the caudal-most portion of the tailbud (boundary marked by dotted line) as excised for detection of bioactive RA. *B*: Percentage of tailbuds excised from embryos of non-diabetic (ND) and manifestly diabetic (MD) mice that have induced different numbers of positively stained cells in the RA reporter cell line ($n = 19$ for ND and 22 for MD from 3 and 4 litters respectively). *C*: Representative figures of excised tailbuds that were placed directly on the RA reporter cells and have induced different numbers of stained cells in the RA reporter cell line.

Figure 4 - Tailbuds of E9 embryos of diabetic mice exhibit a greater magnitude of suppression of key genes for caudal development induced by RA. *A*: Quantification of mRNA levels of various caudal regulatory genes and RA nuclear receptors, normalized to *β-actin*, and expressed relative to ND, which was set as 1, in tailbuds of embryos of non-diabetic (ND) and manifestly diabetic (MD) mice at E9 ($n = 5$ from 5 litters). **$P < 0.01$, Student's *t* test. *B* and *C*: Quantification of mRNA levels of *Cyp26a1* (*B*), and various caudal regulatory genes and RA nuclear receptors (*C*), normalized to *β-actin*, and expressed relative to ND (CON), which was set as 1, in tailbuds of embryos of ND and MD mice 4 h after maternal injection of 50 mg/kg RA (50RA) or vehicle as control (CON)

at E9 (n = 5 from 5 litters). *P < 0.05; **P < 0.01; ***P < 0.001, one-way ANOVA followed by Bonferroni test. Error bars represent mean ± SEM.

Figure 5 - *Cyp26a1* loss of function genotype interacts with diabetic maternal environment to influence RA degrading efficiency and susceptibility to RA teratogenesis. *A*: Whole-mount ISH patterns of *Cyp26a1* expression in *Cyp26a1* heterozygous null (+/-) embryos and their wild-type (+/+) littermates from non-diabetic (ND) and manifestly diabetic (MD) mice at E9. At least 30 embryos from 6-8 litters were examined for each group. Scale bar = 0.25 mm. *B*: Quantification of *Cyp26a1* mRNA, normalized to *β-actin,* and expressed relative to ND (+/+), which was set as 1, in tailbuds of embryos from different genotype-maternal environment combinations at E9 (n = 5 from 5 litters). *C*: *In vitro* RA degrading efficiency, presented as % of RA in the medium being degraded by the tailbud lysate in the absence or presence of 100 nM R115866 (CYP26 inhibitor) (n = 8-13 from 10-14 litters). *D*: Quantification of RA released from individual tailbuds, using a RA reporter cell line, at 3 h after *in vivo* challenge with 25 mg/kg RA (25RA) at E9 (n = 22-28 from 6-7 litters). *E*: Maternal injection of 25 mg/kg RA (25RA) or vehicle as control (CON) at E9. Caudal truncation, measured in terms of the ratio of tail length/crown-rump length (TL/CRL), was examined in E13 embryos (n = 41-62 from 10 litters). *F*: Maternal injection of 40 mg/kg RA (40RA) or CON at E9. Near-term E18 fetuses were examined for renal malformations (n = 11 litters). *P < 0.05; **P < 0.01; ***P < 0.001, one-way ANOVA followed by Bonferroni test. Error bars represent mean ± SEM.

Figure 6 - Pre-conditioning with low dose RA up-regulates *Cyp26a1*, increases RA degrading efficiency, and protects against RA-induced caudal truncation. *A*: Quantification of *Cyp26a1* mRNA, normalized to *β-actin*, and expressed relative to ND (CON), which was set as 1, in tailbuds of E9 embryos from non-diabetic (ND) and manifestly diabetic (MD) mice 2 h after maternal oral feeding with low dose RA of 0.625 mg/kg (0.625RA) or 1.25 mg/kg (1.25RA), or with vehicle as control (CON) ($n = 5$ from 5 litters). *B*: *In vitro* RA degrading efficiency, presented as % of RA in the medium being degraded by the tailbud lysate from embryos with or without preconditioned with 0.625RA ($n = 5$ from 3-5 litters). *C*: Embryos, with or without preconditioned with low dose RA, were maternally challenged with a teratogenic dose of 25 mg/kg RA (25RA) at E9, and examined for caudal truncation, measured in terms of the ratio of tail length/crown-rump length (TL/CRL) at E13 ($n = 34$-60 from 3-5 litters). *$P < 0.01$; **$P < 0.001$, Student's *t* test. [†]$R^2 = 0.900$ and $P < 0.001$; [††]$R^2 = 0.869$ and $P < 0.001$; [†††]$R^2 = 0.610$ and $P < 0.001$; [††††]$R^2 = 0.729$ and $P < 0.001$, linear regression. Dotted line represents no significant difference between the two groups. Error bars represent mean ± SEM.

Figure 7 - Increased susceptibility of embryos of diabetic mice to RA-induced neural tube defects is abolished by pre-conditioning with low dose RA. *A* and *B*: Incidence rates of exencephaly (*A*) and spina bifida (*B*) in E13 *Cyp26a1* heterozygous null (+/-) and wild-type (+/+) embryos from non-diabetic (ND) and manifestly diabetic (MD) mice ($n = 8$-9 litters). Effect of pre-conditioning by oral feeding of low dose 0.625 mg/kg RA (0.625RA) is compared with vehicle-fed control (CON) or no treatment (NT) group, 2 h

prior to *in vivo* challenge with a teratogenic dose of 25 mg/kg RA (25RA) at E8. $*P <$ 0.05; $**P < 0.01$; $***P < 0.001$, one-way ANOVA followed by Bonferroni test. Dotted line represents no significant difference between the two groups. Error bars represent mean ± SEM.
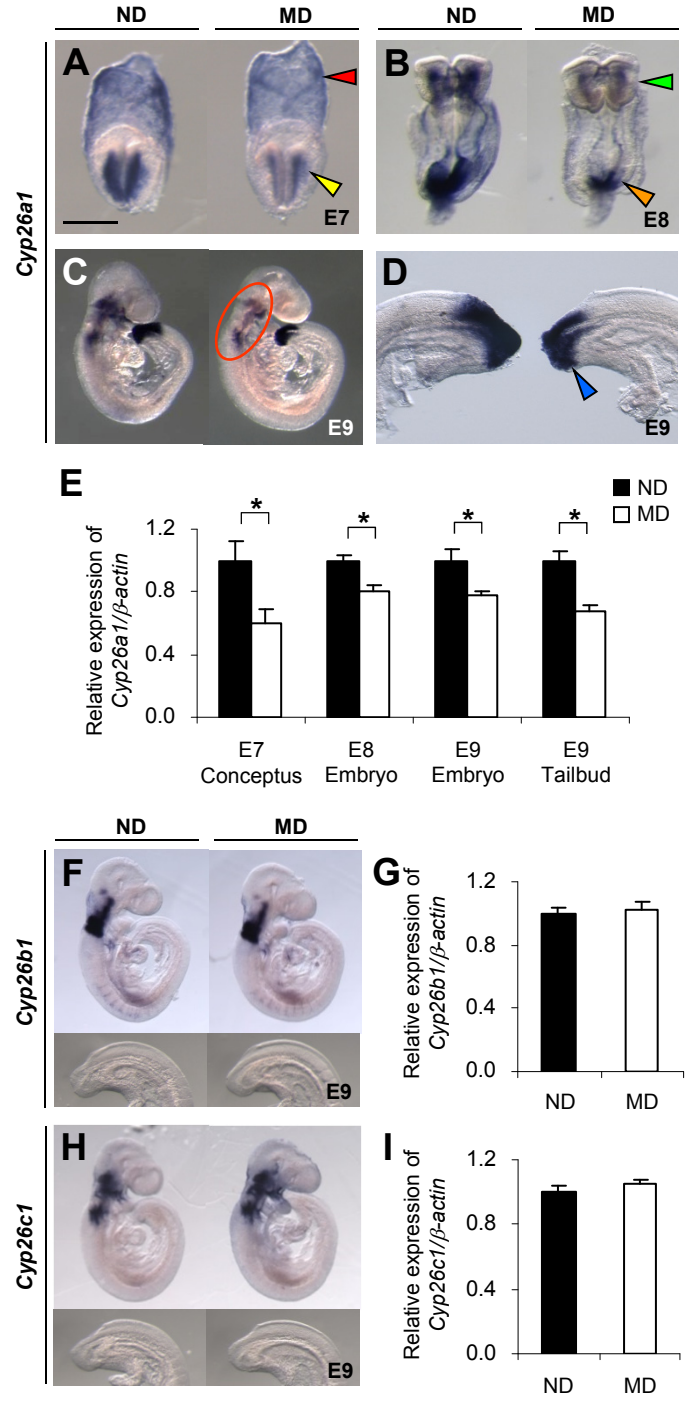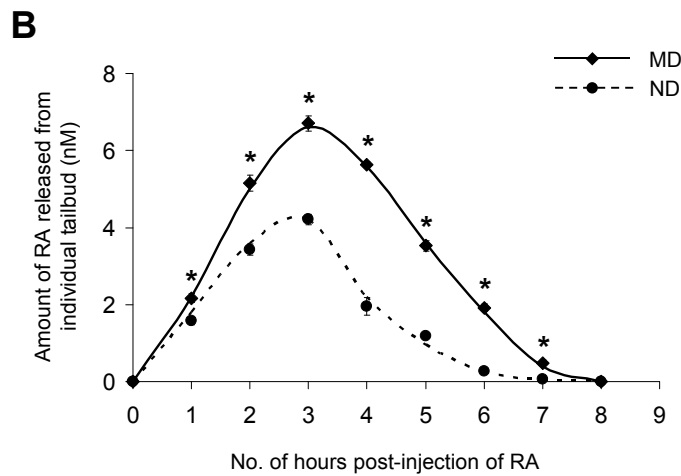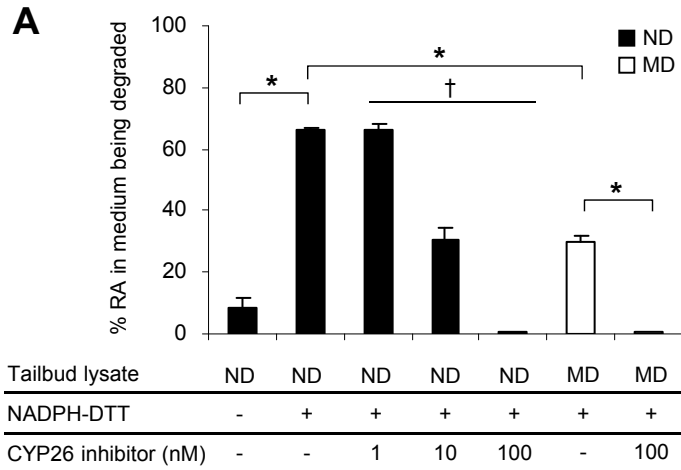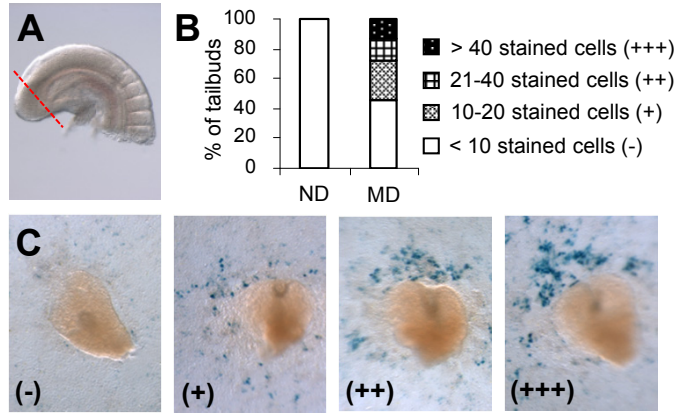
Figure 1

A

Tailbud lysate	ND	ND	ND	ND	ND	MD	MD
NADPH-DTT	-	+	+	+	+	+	+
CYP26 inhibitor (nM)	-	-	1	10	100	-	100

B

Figure 2

A

B

% of tailbuds

100
80
60
40
20
0

ND   MD

■ > 40 stained cells (+++)
⊞ 21-40 stained cells (++)
▨ 10-20 stained cells (+)
☐ < 10 stained cells (-)

C

(-)   (+)   (++)   (+++)

Figure 3

A

Relative expression of *target gene/β-actin*

■ ND
□ MD

1.2, 1.0, 0.8, 0.6, 0.4, 0.2, 0.0

**

Fgf8 *Wnt3a* *Cdx2* *Rarγ* *Rxrα*

B

Relative expression of *Cyp26a1/β-actin*

■ ND (CON)
□ MD (CON)
▨ ND (50RA)
▨ MD (50RA)

14, 12, 10, 8, 6, 4, 2, 0

***
***
***
**
*

Cyp26a1

C

Relative expression of *target gene/β-actin*

1.2, 1.0, 0.8, 0.6, 0.4, 0.2, 0.0

*** ** * *** **

** * **
*

**
*
**

Fgf8 *Wnt3a* *Cdx2* *Rarγ* *Rxrα*

Figure 4

Figure 5

A

B

C
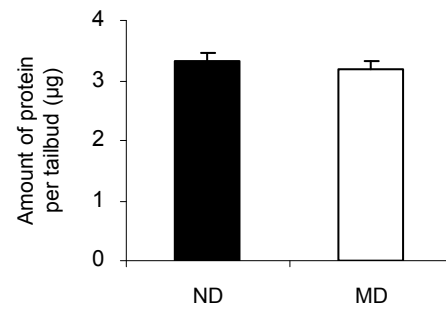
Figure 6

Figure 7

Supplementary Figure 1. A representative standard curve showing the response of the RA reporter cell line to serially diluted RA solutions from 10^{-6}M to 10^{-11}M. A linear dose-response is present from 10^{-7}M to 10^{-10}M. RA concentration of the sample was plotted against the standard curve within the linear range. R^2 represents the coefficient of determination for linear regression analysis.
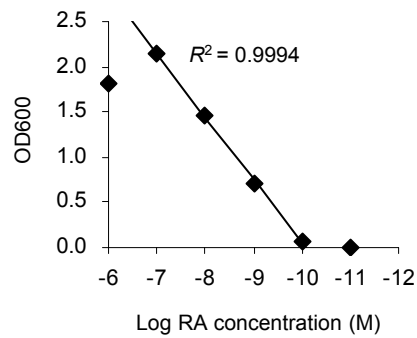
Supplementary Figure 2. RA was stable at 37°C for 24 h. RA was added to the culture medium at a concentration of 10 nM. The medium was either immediately frozen and stored at -80°C ($n = 4$) or incubated at 37°C for 24 h in a 5% CO_2 incubator ($n = 4$). The RA concentrations of the two groups of samples were then determined by the RA reporter cell line. There was no significant degradation of RA in the sample that had been incubated at 37°C for 24 h when compared with the immediately frozen sample.
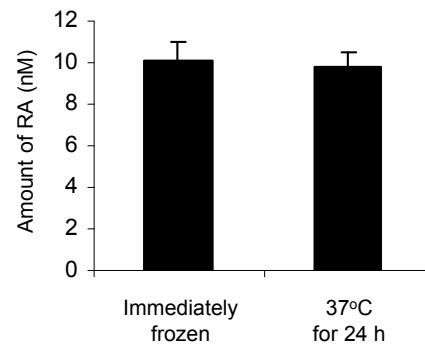
Supplementary Figure 3. No significant difference in the protein content of the excised tailbuds from embryos of non-diabetic (ND) and manifestly diabetic (MD) mice. Total protein in individual tailbuds measured using Bradford assay (n = 18-20 from 3 litters). Error bars represent mean $\pm$ SEM.

Supplementary Figure 4. The midbrain, which does not express any of the three *Cyp26* genes, exhibits no difference in RA levels between embryos of diabetic and non-diabetic mice after RA treatment. *A*: *In situ* hybridization on E9 embryos demonstrates that all three *Cyp26* genes (*Cyp26a1*, *Cyp26b1* and *Cyp26c1*) do not express in the midbrain (MB) with or without (No RA) being maternally treated with 50 mg/kg RA (50RA). Scale bar = 0.4 mm. *B*: Amount of RA in the tailbud and midbrain of E9 embryos 3 h post-injection of 50RA, measured using HPLC (*n* = 7-9 from 7-9 litters). The tailbud of embryos of manifestly diabetic (MD) mice with reduced *Cyp26a1* expression had a significantly greater amount of RA than in embryos of non-diabetic (ND) mice. In contrast, the midbrain, without *Cyp26* expression, showed no difference in the amount of RA between embryos of MD and ND mice. *$P < 0.001$, Student's *t* test. Error bars represent mean ± SEM.
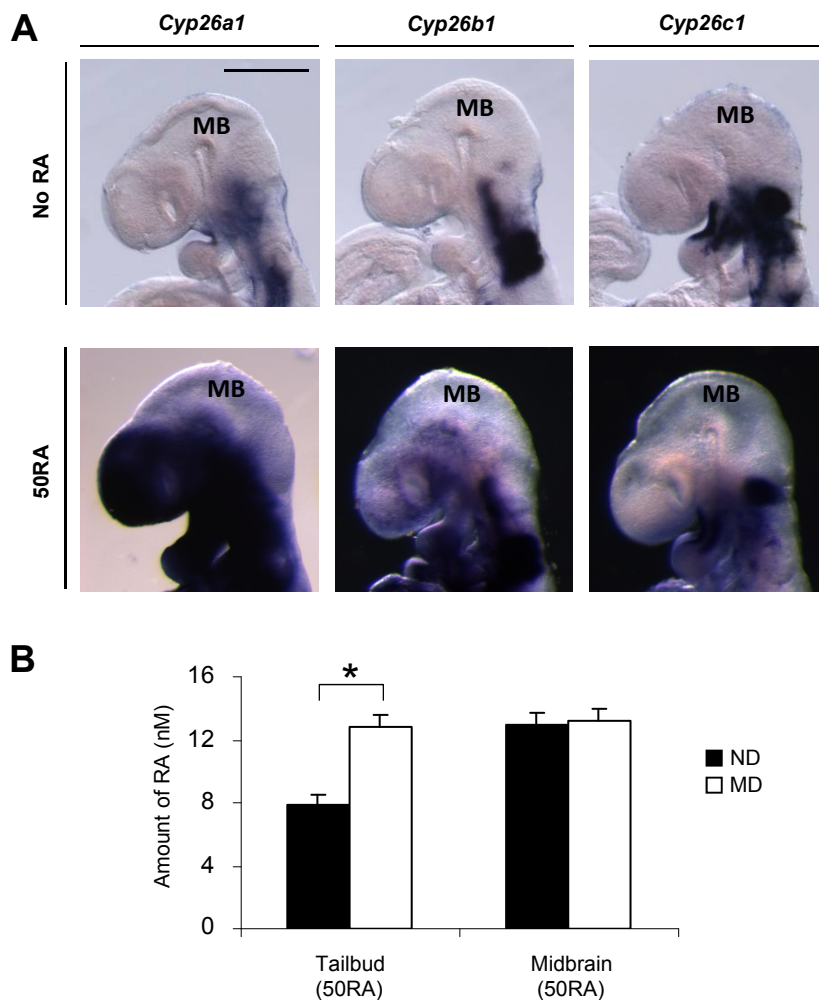
Supplementary Figure 5. Heterozygosity for *Cyp26a1* loss of function exacerbates increased susceptibility to RA-induced caudal truncation in embryos exposed to diabetes. Morphology of the caudal region of E13 *Cyp26a1* heterozygous null (+/-) embryos and their wild-type (+/+) littermates from non-diabetic (ND) and manifestly diabetic (MD) mice that were challenged *in vivo* with 25 mg/kg RA (25RA) or vehicle as control (CON) at E9. Embryos of different genotype-maternal environment combinations showed prominent differences in susceptibility to RA-induced caudal truncation. Scale bar = 0.1 cm.
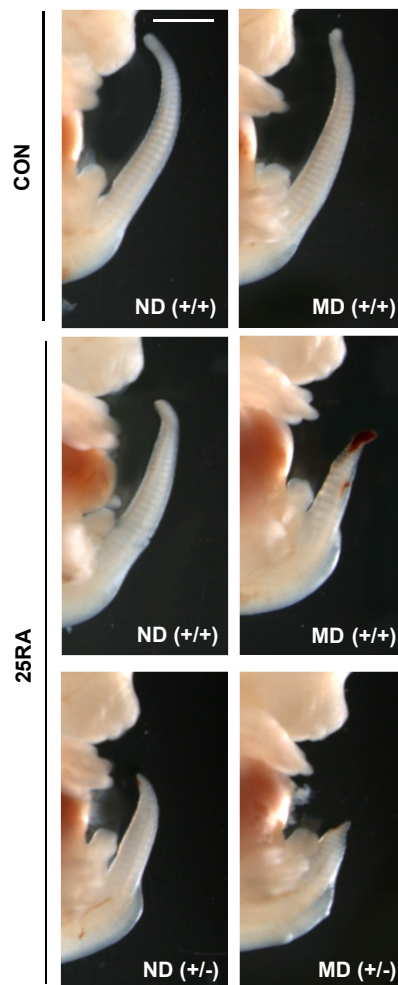
Supplementary Figure 6. Oral feeding of low dose RA does not cause any change in expression of key genes for caudal development. Quantification of mRNA levels of various caudal regulatory genes, normalized to *β-actin,* and expressed relative to ND (CON), which was set as 1, in tailbuds of E9 embryos of non-diabetic (ND) and manifestly diabetic (MD) mice, 2 h after oral feeding with low dose 0.625 mg/kg RA (0.625RA) or vehicle as control (CON) (n = 5 from 5 litters). No significant changes in mRNA levels were associated with low dose RA treatment. *P < 0.05, one-way ANOVA followed by Bonferroni test. Error bars represent mean ± SEM.
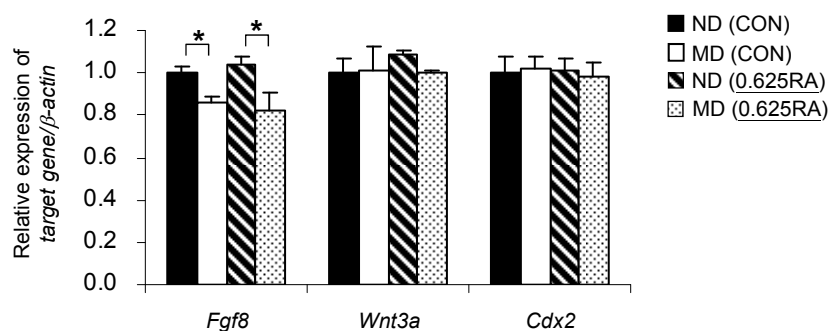
Supplementary Figure 7. Incidence of exencephaly in E13 embryos (ICR ♂ x ICR ♀ genetic background) from non-diabetic (ND) and manifestly diabetic (MD) mice with or without (No RA) *in vivo* challenge with 25 mg/kg RA (25RA) at E8 (*n* = 9-12 litters). In untreated conditions, only 3% of embryos of MD mice developed exencephaly. However, when challenged with 25RA, a dose that only induced exencephaly in 3% of embryos of ND mice, embryos of MD mice were significantly more susceptible to RA teratogenesis and exhibited a nine-fold increase in the incidence rate of exencephaly. *$P < 0.001$, one-way ANOVA followed by Bonferroni test. Error bars represent mean ± SEM.
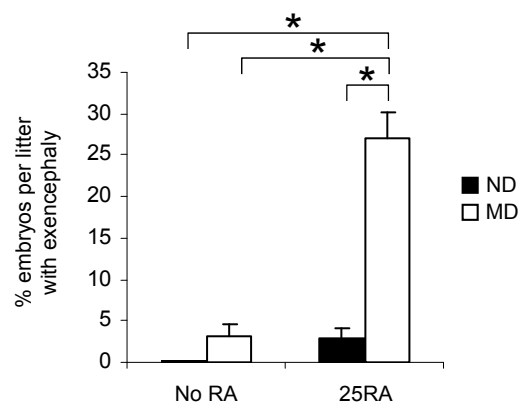
Supplementary Table 1. Blood glucose levels of non-diabetic (ND) and manifestly diabetic (MD) mice before pregnancy and on the day of embryo collection

	<u>ND</u> Before pregnancy	<u>ND</u> Day of embryo collection (E9)	<u>MD</u> Before pregnancy	<u>MD</u> Day of embryo Collection (E9)
Blood glucose levels (mmol/L) mean ± SEM	Not determined	6.08 ± 0.12 (*n* = 12)	21.56 ± 0.32 (*n* = 101)	27.53 ± 0.51* (*n* = 67)

Remarks:
The blood glucose levels of MD mice on the day of embryo collection at E9 were significantly higher than MD mice before pregnancy (*$P < 0.001$, Student's *t* test), with none of them having blood glucose levels lower than 16.7 mmol/L. Similarly, there were hardly any MD mice that exhibited blood glucose levels lower than 16.7 mmol/L on the day of embryo collection at other stages (E8, E13 and E18). These findings supported that embryos of MD mice were exposed to a hyperglycemic milieu throughout development.

Supplementary Table 2. PCR conditions and primer sequences

The PCR conditions included initiation at 95°C for 10 minutes, followed by 40 cycles comprising of denaturation at 95°C for 15 seconds, annealing at 55°C for 30 seconds and extension at 72°C for another 30 seconds. Primers sequences, designed by the Primer Express Software (Applied Biosystems), for detecting various mouse genes were:

Gene	Primer Sequences
β-actin	forward: 5'-TGT TAC CAA CTG GGA CGA CA-3' reverse: 5'-GGG GTG TTG AAG GTC TCA AA-3'
Cdx2	forward: 5'-AAA CTC CAC TGT CAC CCA GT-3' reverse: 5'-CCT GAG GTC CAT AAT TCC AC-3'
Cyp26a1	forward: 5'-CAG TGC TAC CTG CTC GTG AT-3' reverse: 5'-AGA GAA GAG ATT GCG GGT CA-3'
Cyp26b1	forward: 5'-TTC AGT GAG GCA AGA AGA CA-3' reverse: 5'-CTG GGA GGA GGT GCT AAG TA-3'
Cyp26c1	forward: 5'-GGG ACC AGT TGT ATG AGC AC-3' reverse: 5'-AGC CAA CTC CTT CAG CTC TT-3'
Fgf8	forward: 5'-AGA GAT CGT GCT GGA GAA CA-3' reverse: 5'-AAG GGC GGG TAG TTG AGG AA-3'
Rarγ	forward: 5'-AGG CAG CAG ACT GAC CAT TT-3' reverse: 5'-TTC TGG TAG GTG TGC AGC AG-3'
Rxrα	forward: 5'-TCA CCA TCC TCG CCA TCT TT-3' reverse: 5'-CTC CAA ACA GAG GTG CCA TG-3'
Wnt3a	forward: 5'-CTG GCA GCT GTG AAG TGA AG-3' reverse: 5'-GCC TCG TAG TAG ACC AGG TC-3'

Supplementary Table 3. RA in individual tailbuds of embryos of non-diabetic (ND) and manifestly diabetic (MD) mice 3 h post-injection of 50 mg/kg RA at E9, measured using the RA reporter cell line or HPLC

Method of measurement	Amount of RA per tailbud (nM)		
	ND	**MD**	**Difference between ND and MD**
RA reporter cell line	4.21 ± 0.13 $(n = 36)*$	6.71 ± 0.20 $(n = 42)*$	59.38%
HPLC	7.88 ± 0.62 $(n = 7)**$	12.80 ± 0.79 $(n = 9)**$	62.44%

* One tailbud in each sample

** Tailbuds from one litter of embryos were pooled as one sample

Remarks:
The data for the RA reporter cell line was extracted from Fig. 2*B*.
The HPLC experiment was conducted in a separate study to validate the result in Fig. 2*B*. In analyzing the result, it is more relevant to compare the difference between ND and MD groups using the two RA detection methods, rather than the absolute amount of RA in the tailbud.